

Do biological molecular machines act as Maxwell's demons?

Michal Kurzynski & Przemyslaw Chelminiak
*Faculty of Physics, Adam Mickiewicz University,
Umultowska 85, 61-614 Poznan, Poland*

Abstract

In the intention of its creator¹, Maxwell's demon was thought to be an intelligent being, able to perform work at the expense of the entropy reduction of a closed operating system. The perplexing notion of the demon's intelligence was formalized in terms of memory and information processing by Szilard² and subsequent followers^{3,4}, who pointed out that, in order for the total system to obey the second law of thermodynamics, the entropy reduction should be compensated for by, at least, the same entropy increase, related to the demon's information gain on the operating system's state. A non-informational formulation of the problem was proposed by Smoluchowski⁵ and popularized by Feynman⁶ as the ratchet and pawl machine, which can operate only in agreement with the second law. A. F. Huxley⁷ and consequent followers⁸ adopted this way of thinking to suggest numerous ratchet mechanisms for the protein molecular machines' action, but no entropy reduction takes place for these models. More general models of protein dynamics have been put forward⁹⁻¹¹ with a number of intramolecular states organized in a network of stochastic transitions. Here, the computer model of such a network is investigated, displaying, like networks of the systems biology, a transition from the fractal organization on a small length-scale to the small-world organization on the large length-scale¹². This model, when allowing work performance in a variety of ways¹¹, obeys the generalized fluctuation theorem¹³ with entropy reduction and is able to explain a surprising observation to Yanagida and co-workers^{14,15} that the myosin II head can take several steps along the actin filament per ATP molecule hydrolysed. From a broader perspective, the supposition that (i) a similar mechanism of action is characteristic for many intrinsically disordered proteins and (ii) this is the reason for most protein machines to operate as dimers or higher organized structures could be of especial importance.

The biological molecular machines are proteins that operate under isothermal conditions and, thus, are referred to as free energy transducers¹⁶. We understand the word ‘machine’ generally as denoting any physical system that enables two other systems to perform work on each other. The energy processing pathways in any stationary machine, that operates under isothermal conditions¹⁷, are shown in Figure 1, where the notation of the physical quantities being in use is also explained.

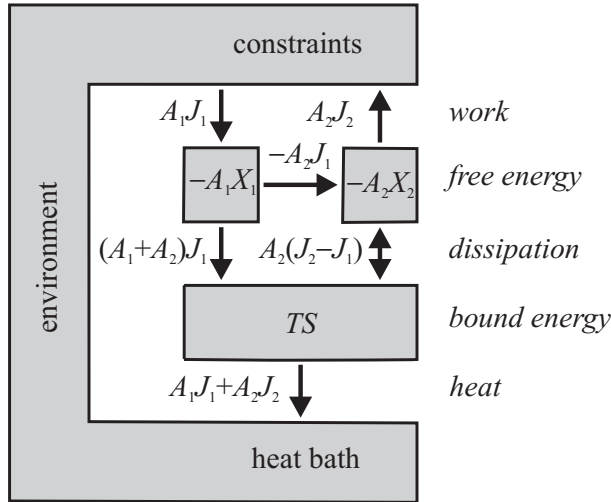


FIG. 1. Energy processing in any stationary (cyclic) isothermal machine. X_i denotes the input ($i = 1$) and the output ($i = 2$) thermodynamic variable (mechanical – displacement, electrical – charge, or chemical – number of distinguished particles), A_i is the conjugate thermodynamic force (mechanical force, electrical or chemical potential difference) and the time derivative, $J_i = dX_i/dt$, is the corresponding flux (velocity, electrical or chemical current). T is the temperature and S is the entropy. We assume the thermodynamic variables to be dimensionless, hence the forces are of energy dimension. By convention, we assume also the thermodynamic fluxes J_1 and J_2 to be of the same sign. Then, one system performs work on the other when the forces A_1 and A_2 are of the opposite sign. The directions of the energy fluxes shown are for $J_1, J_2, A_1 > 0$ and $A_2 < 0$. The direction of the flux, denoted by the forward-reverse arrow, is the subject of this research.

According to the second law of thermodynamics, the net dissipation flux (the internal entropy production rate, multiplied by the temperature) $A_1J_1 + A_2J_2$ must be nonnegative. However, it consists of two components. The first component, $(A_1 + A_2)J_1$, enacted when the

input and output fluxes are tightly coupled and $J_1 = J_2$, must also be, according to the same law, nonnegative. For the present considerations, the sign of the complement $A_2(J_2 - J_1)$ is essential. In the macroscopic systems, the entropy S is additive and can always be divided into the following two parts S_1 and S_2 , relating to the input and output thermodynamic variables X_1 and X_2 , respectively. As a consequence, the flux $A_2(J_2 - J_1)$, which corresponds to S_2 , must also be nonnegative. This means that, for negative A_2 , output flux J_2 should not surpass input flux J_1 . Macroscopically, the second component of the dissipation flux has the obvious interpretation of a slippage in the case of the mechanical machines, a leakage in the case of pumps, or a short-circuit in the case of the electrical machines. However, because of nonvanishing correlations, in the mesoscopic systems like the protein molecular machines, entropy is not additive¹³, and the output flux J_2 can surpass the input flux J_1 ¹¹, which changes the sign of the flux $A_2(J_2 - J_1)$ to the negative. Such a surprising case was observed by Yanagida and his co-workers^{14,15}, who found that the myosin II head can take several steps along the actin filament per ATP molecule hydrolysed.

The relation between the output and input fluxes in biological molecular machines was the topic of our previous studies¹¹. From a theoretical point of view, it is convenient to treat all biological machines, including molecular motors too, as chemo-chemical machines¹⁷. In fact, the external load influences the free energy involved in binding the motor to its track, which can be expressed as a change in the effective concentration of this track. The chemo-chemical machines are enzymes, that simultaneously catalyze two chemical reactions: the free energy-donating input reaction $R_1 \rightarrow P_1$ and the free energy-accepting output reaction $R_2 \rightarrow P_2$. The system considered consists of a single enzyme macromolecule, surrounded by a solution of its substrates, also involving, in the case of the molecular motors, the track. We assume that bimolecular reactions can be considered as effective monomolecular reactions (the concentration of one of the reagents is kept constant) and that there are some relations between the concentration of the reagents and the products¹¹. Then, two independent stationary (nonequilibrium) molar concentrations of the products $[P_1]$ and $[P_2]$, related to the enzyme total concentration $[E]$, are to be treated, respectively, as input and output dimensionless thermodynamic variables considered in Figure 1. The fluxes J_i with the conjugate thermodynamic forces A_i are determined as¹⁶

$$J_i = \frac{d [P_i]}{dt [E]}, \quad \beta A_i = \ln \frac{[P_i]^{\text{eq}} [R_i]}{[R_i]^{\text{eq}} [P_i]}. \quad (1)$$

$\beta = 1/k_B T$, where k_B is the Boltzmann constant, and the superscript eq denotes the corresponding equilibrium concentrations.

On the mesoscopic level, the dynamics of a biological chemo-chemical machine is described by a system of master equations, determining a network of conformational transitions that satisfy the detailed balance condition (the net probability current between the linked pairs of states vanishes), and a system of distinguished states (the ‘gates’) between which the input and output chemical reactions force transitions, that break the detailed balance (Figure 2a). Recently, we proved analytically¹¹ that, for single output gates, when the enzyme has no opportunity for any choice, the ratio J_2/J_1 cannot exceed one. This case also includes the various ratchet models, that assume the input and output gates to coincide⁸, and for which, consequently, the flux $A_2(J_2 - J_1)$ is positive, hence resulting in the entropy increase. The output flux J_2 can only exceed the input flux J_1 in the case of many different output gates.

Our goal is to consider the biological molecular machines with such dynamics. However, very poor experimental support is available for actual conformational transition networks in native proteins. That is why we restrict our attention to model networks here. We have shown¹¹ that the case of many different output gates is reached in a natural way on critical branching trees, extended by long-range shortcuts. Such networks are scale-free and display a transition from the fractal organization on the small length-scale to the small-world organization on the large length-scale¹². A reasonable hypothesis is that the protein conformational transition networks, like the higher level biological networks, the protein interaction network and the metabolic network, have also evolved in the process of a self-organized criticality¹⁸. A network of 100 nodes with such properties is shown in Figure 2b. It was constructed following the algorithm described in the Methods section. The dynamics is also determined there. We have chosen the gates tendentiously, optimizing the value of J_2/J_1 close to 1 for the single gate, and possibly the highest for many gates.

In the mesoscopic machines, the work, dissipation and heat are fluctuating variables and their variations, proceeding forward and backward in time, are related to each other by the fluctuation theorem¹⁹. The probability distribution function for the input and output fluxes, in general, depending on the time period t of determination, satisfies the stationary fluctuation theorem in the Andrieux-Gaspard form²⁰:

$$p(j_1(t), j_2(t))/p(-j_1(t), -j_2(t)) = \exp \beta [A_1 j_1(t) + A_2 j_2(t)] t. \quad (2)$$

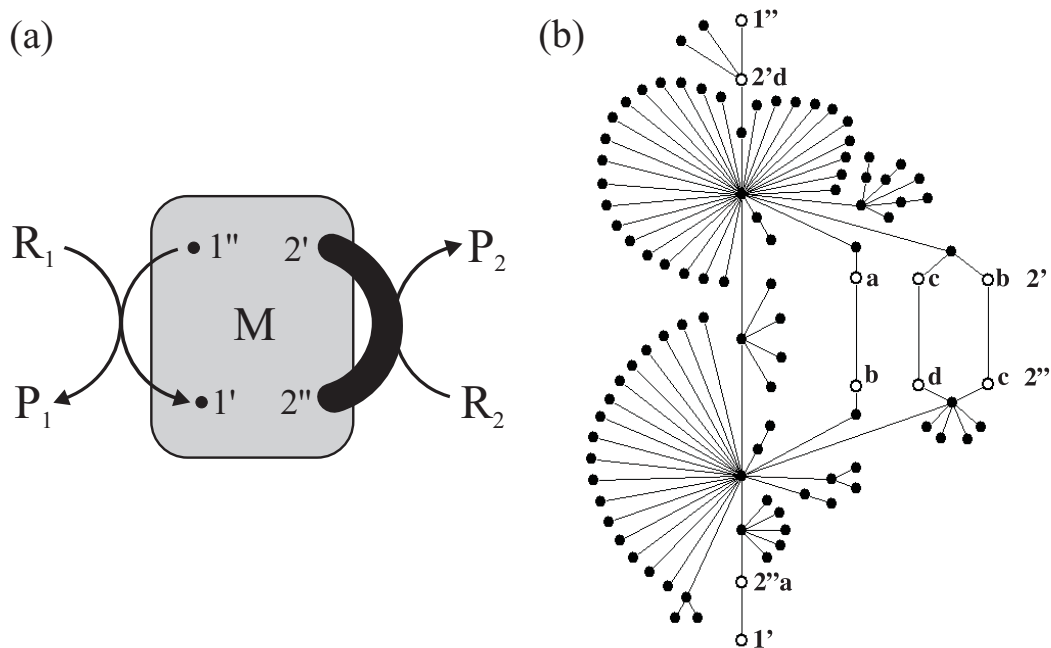


FIG. 2. Kinetics of the enzymatic chemo-chemical machine. **a**, General scheme¹¹. The grey box represents an arbitrary network of transitions between conformational states composing either the enzyme, the enzyme-substrate, or the enzyme-substrates native state. All these transitions satisfy the detailed balance condition. A single pair (the ‘gate’) of conformational states $1''$ and $1'$ is distinguished, between which the input reaction $R_1 \rightarrow P_1$ brakes the detailed balance. Also, a single or a variety (the heavy line) of pairs of conformational states $2''$ and $2'$ is distinguished, between which the output reaction $R_2 \rightarrow P_2$ does the same. All the reactions are reversible; the arrows indicate the directions assumed to be forward. **b**, Exemplifying realization of the network, constructed stochastically following the algorithm described in the Methods section. This one is studied in more detail in the present letter. Note two hubs, the states of the lowest free energy, that can be identified with the two main conformations of the protein machine, e.g., ‘open’ and ‘closed’, or ‘bent’ and ‘straight’, usually the only occupied sufficiently high to be notable under equilibrium conditions. The single pair of the output transition states chosen for the simulations is $(2''a, 2'd)$. The alternative four output pairs $(2''a, 2'a)$, $(2''b, 2'b)$, $(2''c, 2'c)$, and $(2''d, 2'd)$, are chosen tendentially to lie one after another.

This can be equivalently rewritten as the Jarzynski equality¹⁹

$$\langle \exp(-\sum_i \beta A_i \mathcal{J}_i(t)t) \rangle = \langle \exp(-\sigma) \rangle = 1. \quad (3)$$

p is the joint probability distribution function for the statistical ensemble of the fluxes, and $\langle \dots \rangle$ is the average over that ensemble. $\mathcal{J}_i(t)$ denotes the random variable of the mean net flux over the time period t , $i = 1, 2$, and $j_i(t)$ denotes the particular value of this flux with J_i in Figure 1 being the corresponding average for $t \rightarrow \infty$. σ has the meaning of a dimensionless entropy production, and the concavity of the exponential causes the second law of thermodynamics, $\langle \sigma \rangle \geq 0$, to be a consequence of (3).

From the point of view of force A_2 , subsystem 1 carries out work on subsystem 2 while subsystem 2 carries out work on the environment. Jointly, the effective work $A_2(J_2 - J_1)$ is performed on or by subsystem 2 (see Figure 1). From the fluctuation theorem (2) for the whole system, the generalized fluctuation theorem for the difference $j_2 - j_1$ follows in the logarithmic form:

$$\begin{aligned} \ln p(j_2 - j_1)/p(-j_2 + j_1) &= \beta A_2(j_2 - j_1)t \\ + \int dj_1 p(j_1) &[\ln p(-j_2 + j_1 | -j_1)/p(-j_2 + j_1) - \ln p(j_2 - j_1 | j_1)/p(j_2 - j_1)]. \end{aligned} \quad (4)$$

We introduced conditional probabilities here and assumed the very input flux j_1 to satisfy the usual fluctuation theorem with respect to the force $A_1 + A_2$ (see Figure 1). Independently on the approximation, the Jarzynski equality corresponding to (4) can be written as¹³

$$\langle \exp(-\sigma - \iota) \rangle = 1. \quad (5)$$

ι , the fluctuating integral from Eq. (4), has the meaning of some information gain in nats (the natural logarithm is used instead of the binary logarithm). A consequence of (5) is a generalized version of the second law of thermodynamics^{13,25}

$$\langle \sigma \rangle \geq -\langle \iota \rangle. \quad (6)$$

This allows the entropy production $\langle \sigma \rangle$ to be negative if the information gain $\langle \iota \rangle$ is positive, and describes the case of Maxwell's demon exactly.

We performed Monte Carlo simulations of random walk, described by the respective master equations (see the Methods section), on the network shown in Figure 2b, with both the single and the fourfold output gate. We found that

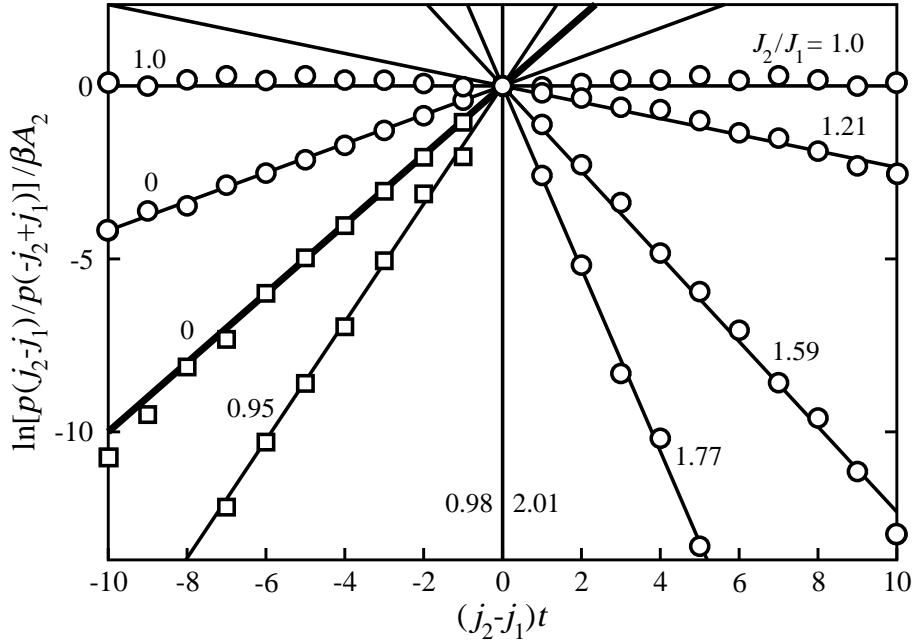


FIG. 3. Generalized fluctuation theorem dependence (4) that was found in Monte Carlo simulations for the network which was shown in Figure 2b with the single output gate (the squares) and the fourfold output gate (the circles). The dynamics of the model was that described in the Methods section. We assumed $\beta A_1 = 1$ and a few negative values of βA_2 determining the average difference $J_2 - J_1$ of the output and input fluxes, thus, the ratio J_2/J_1 noted in the figure. For clear presentation of the contribution from the information transfer, the both sides of the dependence (4) were divided by the (negative!) coefficient βA_2 . The results of each simulation were obtained on the whole axis of the fluctuating difference $j_2 - j_1$ but in the figure, they are presented only on the left from zero for the negative average differences $J_2 - J_1$ (the ratio $J_2/J_1 < 1$), and on the right from zero for the positive average differences $J_2 - J_1$ (the ratio $J_2/J_1 > 1$). The thick, solid line corresponds to the lack of information transfer in Eq. (4), which takes place for the force $\beta A_2 = -0.670$, that stalls the flux through the single output gate ($J_2/J_1 = 0$). The same effect of stalling the flux through the fourfold output gate is reached for $\beta A_2 = -0.173$, but this needs a non-zero information gain (the line with a lower slope). The entropy production is completely compensated for by the information gain for $\beta A_2 = -0.108$, when the difference $J_2 - J_1$ reaches the value of 0 ($J_2/J_1 = 1$, the horizontal line). The vertical line ($\beta A_2 = 0$) corresponds to the maximum value of J_2/J_1 both for the fourfold output gate (on the right from zero), and the single output gate (on the left from zero).

- (i) the two-dimensional probability distribution function $p(j_1(t), j_2(t))$ satisfies the Andrieux-Gaspard fluctuation theorem (2) for t longer than the mean equilibration time between the nearest neighbors,
- (ii) the one-dimensional marginal $p(j_1)$ satisfies with a good approximation the similar fluctuation theorem with respect to the force $A_1 + A_2$.
- (iii) the logarithm of the diagonal marginals ratio $p(j_2 - j_1)/p(-j_2 + j_1)$ can be described by the generalized fluctuation theorem formula (4) with both the component terms linearly depending on the difference $j_2 - j_1$,
- (iv) the results of the simulations for the case of tight coupling, $J_2 = J_1$, display exceptionally large fluctuations.

The generalized fluctuation theorem dependences are presented in Figure 3 for a few chosen negative values of βA_2 that determine the average difference $J_2 - J_1$ of the output and input fluxes. The thick, solid line in this figure corresponds to the first term to the right-hand side of Eq. (4). We see that the correction, originating from the second term, can be very large indeed. For the single output gate, when the system has no opportunity of any choice, this correction is always negative, that corresponds to information loss. For many output gates, information gain, resulting from the possibility of a choice, reduces the effects of the entropy production in part, until the limit of the tight coupling, $J_2 - J_1 = 0$, ($J_2/J_1 = 1$), above which information gain prevails, that results in the entropy reduction. The simulation data are presented in such a way that the transition from the entropy production to entropy reduction might be clearly seen. Note that the limit of the tight coupling can be also reached for the single output gate, but it only is enacted for the negligible slippage, and is not related to any entropy reduction.

To summarize, we studied the fluctuations of the flux difference $J_2 - J_1$, which is the time derivative of the variable $X_2 - X_1$. This variable characterizes not the energy but the organization of the system (in the case of the macroscopic mechanical machines, it could be, for example, the possibly shifting connection of a component wheel to its axle). The main conclusion of the study is that the free energy processing has to be distinguished from the organization processing (Figure 4). Both free energy and organization are functions of the state of the system. On the contrary, information I , entropy production, denoted in the

figure as S , and cost C , the balance of these two quantities, like the entire work W and dissipation D are functions of the process. The quantity I is the product of the dimensionless quantity ι and the Boltzmann constant k_B .

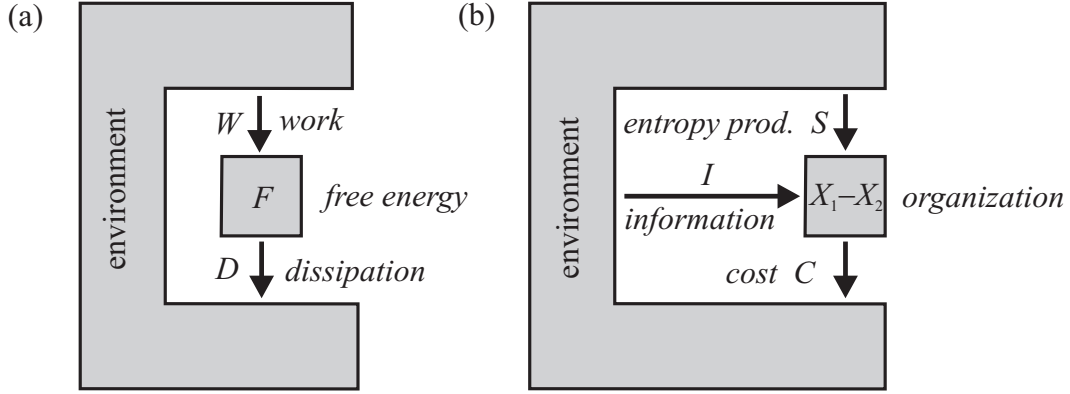


FIG. 4. Free energy (a) and organization (b) processing in any physical system, participating in a stationary process under isothermal conditions. See the text for the discussion.

For the systems operating under stationary isothermal conditions, the first and second laws of thermodynamics

$$W = D \geq 0 \quad (7)$$

hold for the free energy processing. For the organization processing, the generalized first and second laws of thermodynamics can be written as

$$S + I = C \geq 0. \quad (8)$$

For the macroscopic machines as well as the mesoscopic enzymatic machines with a single output gate, I is negative, so S must always be positive. However, for some enzymatic machines with multiple output gates, we here showed that I can be positive, and thus, S can be negative (the reduction of the entropy instead of the production) when only $I \geq C$. Only such biological molecular machines may be said to act as Maxwell's demons. In general, Maxwell's demon is a physical system that is complex enough to make a choice and to collect information. So is also any quantum system entangled with the rest of the Universe, including an observer²¹.

As mentioned earlier¹¹, our model is able to explain a surprising observation to Yanagida and his co-workers that the myosin II head can take several steps along the actin filament

per ATP molecule hydrolysed^{14,15}. It is likely that the mechanism of the action of the small G-proteins that have a common ancestor with the myosin²² and an alike partly disordered structure after binding the nucleoside triphosphate²³ is, after a malignant transformation, similar. Presumably, also, natively disordered transcription factors actively look and not passively for their target on the genome²⁴.

Note that we do not distinguish the system and the memory (observer) as Sagawa and Ueda¹³ do after the Szilard understanding of Maxwell's demon². Depending on the context, Figure 4b can represent the action of either the system, the memory, or both. For the last interpretation that we share with Deffner and Jarzynski²⁵, the case when the information gain compensates exactly for the entropy production (the cost $C = 0$), is exceptional. Our simulation clearly points out (Figure 3) that such a case happens for the tight coupling, $J_2 - J_1 = 0$, and, thus, also for $S = 0$ simultaneously with $I = 0$. Exceptionally large fluctuations of the flux differences $j_2 - j_1$, observed by us, suggest that the transition from entropy production to entropy reduction has the character of a phase transition. This case is the optimum in the sense that the organization cost of the total system is than zero. We cannot, however, forget that from the energetic point of view, the dissipation $(A_1 + A_2)J_1$ still occurs (see Figure 1), albeit it tends to zero in the quasi-static limit $J_1 \rightarrow 0$.

The case of the tight coupling occurs in a natural way in systems composed of two subsystems: the very operating system and a memory, between which a feedback control^{4,13,25} is realized. Both subsystems exchange information with each other. Transfer of information from the operating system to memory is the measurement process. Transfer of information from the memory to the operating system is the control. No net information transfer with the environment is necessary, $I = 0$. The result is an entropy reduction of the operating system, that can be used for some work performance, and, simultaneously, the equal entropy production in memory, that must be erased at the expense of the same amount of work. No net entropy production takes place, $S = 0$. There are convincing arguments, for instance, for the kinesin motor²⁶ and the quinol:cytochrome c oxidoreductase²⁷, that a feedback control^{13,25} with the net $I = 0$ and $S = 0$ is achieved in dimeric protein complexes which are composed of two identical monomers, alternatively playing the role of the observer (memory) and the controlled unit.

METHODS

The algorithm of constructing the stochastic scale-free fractal trees was adopted after Goh et al.²⁸. Shortcuts, though more widely distributed, were considered by Rozenfeld, Song and Makse¹². The network of $n = 100$ nodes in Figure 2b is too small to determine its scaling properties, but a similar procedure of construction applied to 10^5 nodes results in a scale-free network that is fractal on a small length-scale and a small world on a large length-scale. To provide the network with stochastic dynamics, we assumed the probability of changing a node to any of its neighbours to be the same in each random walking step. Consequently, the transition probability to the neighbouring node is inversely proportional to the number of links (the output node degree)¹¹. Following the detailed balance condition, the free energy of a given node is proportional to its degree. The larger the number of links, the higher the equilibrium occupation probability of the node. Thus, the lower its free energy. The most stable conformational substates are the hubs. The forward external transition probabilities, determined by the stationary concentrations $[P_i]$, were assumed to equal $(20 p_i^{\text{eq}})^{-1}$ per random walking step, p_i^{eq} denoting the equilibrium occupation probability of the initial input or output node, $i = 1, 2$. The corresponding backward external transition probabilities were modified by the detailed balance breaking factors $\exp(-\beta A_i)$. We performed Monte Carlo simulations of the random walk in 10^{10} computer steps on the network shown in Figure 2b with both the single and the fourfold output gate. The mean equilibration time between the nearest neighbors equals $2(n - 1) = 198$ computer steps for the network and the dynamics considered. We chose the optimal time of averaging $t = 10^5$ random walking steps for the single gate and $t = 10^3$ random walking steps for the fourfold gate. From the two-dimensional distributions $p(j_1, j_2)$, the marginals $p(j_1)$ and $p(j_2 - j_1)$ were determined. We discarded the rare results for the higher values of $j_2 - j_1$ as being burdened with statistical error too large.

¹ Maxwell, J. C. *Theory of Heat*, Logmans: London, 1871.

² Szilard, L. Z. On the decrease of entropy in a thermodynamic system by the intervention of intelligent beings. *Z. f. Phys.* **1929**, *53*, 840-856.

- ³ Leef, H. S.; Rex, A. F., eds. *Maxwell's Demon 2: Entropy, Classical and Quantum Information, Computing*. Institute of Physics Publishing: Bristol and Philadelphia, 2003.
- ⁴ Lu, Z.; Mandal, D.; Jarzynski, C. Engineering Maxwell's demon. *Physics Today* **2014**, *67*, 60-61.
- ⁵ Smoluchowski, M. Experimentell nachweisbare der üblichen Thermodynamik widersprechende Molekularphänomene. *Phys. Z.* **1912**, *13*, 1069-1080.
- ⁶ Feynman, R. P.; Leighton, R. B.; Sands, M. *The Feynman Lectures on Physics*, vol. 1, Addison-Wesley, Reading, Massachusetts, 1963, chap. 46.
- ⁷ Huxley, A. F. Muscle structure and theories of contraction. *Prog. Biophys. Biophys. Chem.* **1957**, *7*, 255-318.
- ⁸ Howard, J. Motor proteins as nanomachines: the roles of thermal fluctuations in generating force and motion. In *Biological Physics – Poincaré Seminar 2009*, Duplainer B., Rivasseau, V., eds. (Springer, Basel, 2010), pp 47-61.
- ⁹ Lacoste, D.; Mallick, K. Fluctuation relations for molecular motors. In *Biological Physics – Poincaré Seminar 2009*, Duplainer B., Rivasseau, V., eds. (Springer, Basel, 2010) pp 61-88.
- ¹⁰ Kurzynski, M. A synthetic picture of intramolecular dynamics of proteins. Towards a contemporary statistical theory of biochemical processes. *Progr. Biophys. Mol. Biol.* **1998**, *69*, 23-82.
- ¹¹ Kurzynski, M.; Torchala, M.; Chelminiak, P. Output-input ratio in thermally fluctuating biomolecular machines. *Phys. Rev. E* **2014**, *89*, 012722.
- ¹² Rozenfeld, H. D.; Song, C.; Makse, H. A. Small-world to fractal transition in complex networks: A renormalization group approach. *Phys. Rev. Lett.* **2010**, *104*, 025701.
- ¹³ Sagawa, T.; Ueda, M. Nonequilibrium thermodynamics of feedback control. *Phys. Rev. E* **2012**, *85*, 021104.
- ¹⁴ Kitamura, K.; Tokunaga, M.; Iwane, A. H.; Yanagida, T. A single myosin head moves along an actin filament with regular steps of 5.3 nanometers. *Nature* **1999**, *397* 129-134.
- ¹⁵ Kitamura, K.; Tokunaga, M.; Esaki, S.; Iwane, A. H.; Yanagida, T. Mechanism of muscle contraction based on stochastic properties of single actomyosin motors observed in vitro. *Biophysics* **2005**, *1*, 1-19.
- ¹⁶ Hill, T. L. *Free Energy Transduction and Biochemical Cycle Kinetics*; Springer: New York, 1989.
- ¹⁷ Kurzynski, M. *The Thermodynamic Machinery of Life*; Springer: Berlin, 2006, chaps. 3, 8.

- ¹⁸ Sneppen, K.; Zocchi, G. *Physics in Molecular Biology*; Cambridge University Press: New York, 2005, chaps. 8, 9.
- ¹⁹ Jarzynski, C. Nonequilibrium work relations: foundations and applications. *Eur. Phys. J. B* **2008**, *64*, 331-340.
- ²⁰ Andrieux, D.; Gaspard, P. Fluctuation theorem for currents and Schnakenberg Network Theory. *J. Stat. Phys.* **2007**, *127*, 107.
- ²¹ Zurek, W. H. Decoherence, einselection, and the quantum origins of the classical. *Revs Mod. Phys.* **2003**, *75*, 715.
- ²² Kull, F. J.; Vale, R. D.; Fletterick, R. J. The case for a common ancestor: kinesin and myosin motor proteins and G proteins *J. Muscle Res. Cell Motil.* **1998**, *19*, 877-886.
- ²³ Kosztin, I.; Bruinsma, R.; O'Lague, P.; Schulten, K. Mechanical force generation by G proteins. *Proc. Natl. Acad. Sci. USA* **2002**, *99*, 3575-3580.
- ²⁴ Tafvizi, A.; Huang, F.; Fersht, A. R.; Mirny, L. A.; van Oijen, A. M. A single-molecule characterization of p53 search on DNA. *Proc. Natl. Acad. Sci. USA* **2011**, *108*, 263-268.
- ²⁵ Deffner, S.; Jarzynski, C. Information processing and the second law of thermodynamics: An inclusive, Hamiltonian approach. *Phys. Rev. X* **2013**, *3*, 041003.
- ²⁶ Bier, M. The stepping motor protein as a feedback control ratchet. *BioSystems* **2007**, *88*, 301-307.
- ²⁷ Swierczek, M. *et al.* An electronic bus bar lies in the core of cytochrome bc₁. *Science* **2010**, *329*, 451-454.
- ²⁸ Goh, K. I.; Salvi, G.; Kahng, B.; Kim, D. Skeleton and fractal scaling in complex networks. *Phys. Rev. Lett.* **2006**, *96*, 018701.

Acknowledgements MK thanks Yaşar Demirel and Hervé Cailleau for discussing the problem in the early stages of the investigation.